DEFENCE AND CIVIL INSTITUTE
OF ENVIRONMENTAL MEDICINE

Canada

December 1985

DCIEM No. 85-R-50

MODELLING THE UPTAKE OF INERT GAS IN ANESTHETIZED RABBITS UNDER HYPERBARIC CONDITIONS

P. Tikuisis

R.Y. Nishi

P. Giry*

Defence and Civil Institute of Environmental Medicine
1133 Sheppard Ave. W., P.O. Box 2000
Downsview, Ontario, Canada M3M 3B9

* Centre d'Etude et de Recherches Biophysiologiques Appliquées à la Marine
Toulon, France

DEPARTMENT OF NATIONAL DEFENCE - CANADA

ABSTRACT

The rate of uptake of inert gas was modelled mathematically to analyze the measured uptake of *He* and N_2 in the arterial and mixed venous blood of anesthetized rabbits under hyperbaric conditions. These gases were breathed separately and switched isobarically, and were measured *in vivo* with a fast response mass spectrometer probe. Various compartmental models were applied to analyze the rate of inert gas uptake in the rabbit. The one-compartment model suggested that the uptake of N_2 in the whole body was perfusion-limited; however, this was not the case for *He* uptake. When a two-compartment model of fat and non-fat components was applied, the prediction of the fat composition of the rabbit was found to be unrealistically high. A four-compartment perfusion-limited model, which included the alveolar region, greatly overpredicted the saturation rates for both *He* and N_2 in blood. When the alveolar region was excluded in a three-compartment model, good agreement was obtained with the measured values of the mixed venous blood gas tension for *He* uptake. The same model, however, did not give as good agreement for N_2 uptake. It appears that, although a three-compartment model is suitable for the analysis of *He* uptake, a one-compartment model is more suitable for N_2 uptake.

Table of Contents

Introduction 1

Methods 1

Results 2

Analysis 3

- One-Compartment Model 3
- Two-Compartment Model 4
- Four-Compartment Model 5
- Three-Compartment Model 6

Discussion 7

Summary 8

Recommendations 8

Acknowledgements 8

References 9

List of Figures 11

Appendix 18

INTRODUCTION

The transport of inert gases into and out of the various tissues of the body is a prime concern in the research of decompression sickness. Decompression sickness is caused by the formation of gas bubbles which can occur in tissues that are supersaturated with gas. The degree of gas supersaturation in the tissues depends upon the rate of gas exchange between tissue and blood; the faster the exchange of gas during the decompression, the less likely will bubbles form in tissue. Over the years, many investigators have attempted to model the mechanism of this gas exchange. Mathematical models range from the perfusion-limitation approach to the diffusion-limitation approach.

Perfusion-limited models assume that the blood perfusion rate for tissues determine the gas exchange rate for those tissues (1-2). This approach has had some experimental support for dealing with certain tissues (2-4), and recently it has been applied to predict tissue gas tensions during isobaric inert gas exchange (5).

Diffusion-limited models assume that the gas exchange rate in tissue is limited by one or all of a number factors including blood-tissue barriers (6-7) and both the radial and axial diffusion of gas (8). The controversy over whether the perfusion-limitation or the diffusion-limitation approach is valid depends upon the specific tissue in question (7,9-10). Although it appears that the diffusion-limitation approach has merit in modelling the finer details of gas exchange between tissue and blood (11), the perfusion-limitation approach is more suitable for the analysis of whole body gas exchange (4).

Various methods are available for the experimental measurement of the inert gas uptake in the body. These involve mass spectrometry where the dissolved gas can be sampled directly and continuously in either tissue or blood (12); radioactive imagery which is suitable for measuring the uptake of radioactive gas in surface tissues (13); and gas chromatography which requires blood sampling (14).

In this paper, the uptake of inert gas during an isobaric switch between N_2 and He in anesthetized rabbits is examined by applying various compartmental models of inert gas exchange to data obtained by mass spectrometry. This data is limited to the measurement of inert gas in either the arterial or venous blood. One- and two-compartment models were applied which were based on a mass balance approach and not on perfusion or diffusion limitations. Three- and four-compartment models were applied in which perfusion-limitation was assumed. All models are based on the arterio-venous difference in inert gas tension and since only the arterial or venous blood was sampled, approximations are made about the other. The goodness of fit of the models to the data is subject to these approximations.

METHODS

Rabbits of approximately 3 kg mass were anesthetized (1 gm urethan per kg body mass) and prepared in the following way. First, on each animal, a tracheotomy was performed and a cannula, connected to two one-way low resistance valves, was inserted (see Fig.1). The inspiratory side of the cannula was connected to a remotely-controlled two-way valve through which either the chamber gas containing 90% N_2 and 10% O_2 or gas from an external tank containing 90% He and 10% O_2 could be breathed. The resistance to breathing was about 1 cm $H_2O/l/s$. Artificial ventilation was not applied in these experiments. The expiratory side was connected to a reservoir which was emptied in such a way that the expired gases did not contaminate the chamber gas. The chamber gas was circulated through a loop (not shown) containing soda lime to remove CO_2 and the absence of CO_2 was verified with an infrared gas analyzer.

A mass spectrometer (Riber QSX 200) was used for the direct continuous measurement of dissolved blood gases (15). The gas sampling probe was constructed of a nickel housing of about 1.0 cm in length and 0.5 mm in diameter and with a porosity of about 1.0 μm. The tip of the housing was covered with a silastic membrane, permeable to gas, but not to liquid (see Ref.15 for greater detail). The response times for both *He* and N_2 have been measured in a saline solution at 40° C and 5 bar. For *He*, 63% of full scale response occured in 10.0 ± 0.2 s, and for N_2, 63% of full scale response occured in 24.0 ± 1.0 s (16).

The blood gases were measured in either the arterial or venous sides of the rabbit (16-17). For the arterial gas tension measurements, the mass spectrometer probe was inserted through the femoral artery and moved about 10 cm forward until positioned in the aorta (16). Post-mortem verification on the probe position was performed. For the mixed venous gas tension measurements, the mass spectrometer probe was inserted through the jugular vein and moved about 15 cm into the superior vena cava at the junction of the right atrium, again with post-mortem verification (17). Reactive error due to the depletion of gas in the vicinity of the probe position was minimized by choosing sites of large blood flow.

After the preparation, each rabbit was individually placed into the chamber and subjected to the following protocol. First, the hyperbaric chamber, 0.8 m^3 in volume, was pressurized with a gas mixture of 90% N_2 and 10% O_2. The chamber pressure was maintained at 5.0 ± 0.1 bar. A period of 90 min was allowed for system equilibration, during which the rabbit breathed the chamber gas mixture. After this period of time, the inspired gas was switched isobarically - within one breath - to a mixture of 90% *He* and 10% O_2, also at a total pressure of 5.0 bar. During this phase, the level of *He* in the blood was measured until no significant variation (i.e. 0.1% of full range) occurred during a 30 min period. When it was determined that equilibrium had taken place, the inspired gas mixture was returned to the chamber mixture of 90% N_2 and 10% O_2. During this phase, the uptake of N_2 in the blood was measured.

The chamber temperature was maintained at 29.0 ± 0.5°C throughout the experiment. The body temperature of the rabbits were monitored and found to be steady at 40.0 ± 0.5°C before and during the experiment.

RESULTS

The values of the measured gas tensions, Π, of *He* and N_2 during uptake are shown in normalized form (indicated by a prime) in Fig. 2. The normalized arterial gas tensions, Π'_a, are the mean of values measured in the aortas of five rabbits. The normalized mixed venous gas tensions, Π'_v, are the mean of values measured in the right atriums of a second group of six rabbits.

It was found that the inert gases did not saturate the arterial blood instantaneously when the rabbit was exposed to the rapid isobaric change in inhaled gas composition. Half-times and 99% saturation times for *He* uptake in the arterial blood were approximately 1.2 min (50%) and 17 min (99%). For N_2, they were 2.4 min (50%) and 55 min (99%).

Corresponding saturation times for mixed venous gas uptake were approximately 3.6 min (50%) and 95 min (99%) for *He*, and 15 min (50%) and 75 min (99%) for N_2. In Fig.2, *He* uptake is shown to be faster than N_2 uptake in the mixed venous blood until about 97% saturation; thereafter, *He* uptake proceeds at a slower rate than does N_2. Aside from possible measurement error due to poor precision near saturation, certain theoretical explanations are offered further on (see DISCUSSION).

ANALYSIS

The rate of inert gas uptake in the body is determined by the arterio-venous difference in gas tension. This difference has not been measured directly; however, the arterial gas tensions for one group of rabbits and the mixed venous gas tensions for a second group of rabbits have been measured under the same experimental conditions. Although neither the extent nor the effect of the physiological variations between the two groups of rabbits can be predicted, these differences should be reduced by using mean values of the blood gas tensions. The approach taken here is to examine which compartmental model best predicts these mean values, and having identified such a model, it could be used to predict the difference in the arterio-venous gas tension and thus the rate of inert gas uptake.

One-Compartment Model

The theoretical investigation begins by examining the exchange of gas between blood and a single compartment modelling the whole animal. Although simplistic in approach, the techniques involved provide the fundamental concepts pertinent to the development of more realistic, though more complex, compartmental models for determining inert gas exchange.

The one-compartment model is schematically represented in Fig. 3a. Gas enters the compartment through the arterial blood and emerges through the venous blood. The extravascular region is assumed to be homogeneous. The conservation of mass is applied to analyze the uptake of gas in the compartment.

The rate of change of gas mass, dM, in the compartment can be expressed as

$$dM = (C_a - C_v)Q dt, \tag{1}$$

where C_a and C_v are the gas concentrations in the arterial and mixed venous blood, respectively, and Q is the volumetric blood flow rate through the compartment. By introducing the Ostwald solubility coefficient (18), L, and dividing through by the compartment volume, V, Eq. 1 becomes

$$dM/V = (L_b/kT)(\Pi_a - \Pi_v)Q dt, \tag{2}$$

where the subscript b refers to a property of the blood, k is the Boltzmann gas constant, T is the temperature, Π is the inert gas tension, and Q is the blood perfusion rate. The first term in Eq. 2 is simply the rate of change of gas mass in the compartment per unit volume and can be rewritten in terms of the gas tension. Therefore, the change in the compartmental inert gas tension is expressed by

$$d\Pi = \lambda Q(\Pi_a - \Pi_v)dt, \tag{3}$$

where λ is the blood:compartment partition coefficient, i.e. L_b/L.

Normalized values of the gas tensions, denoted by a prime, are obtained by dividing the gas tension values by the saturation pressure. Therefore, a compartment not exposed to the inert gas has an initial value of zero, i.e.

$$\Pi'(0) = 0 \tag{4}$$

and, upon complete saturation of the inert gas, the compartment gas tension has a final normalized value of unity, i.e.

$$\Pi'(\infty) = 1. \tag{5}$$

If the inert gas tensions in the arterial and mixed venous blood are known, then the normalized rate of uptake of the inert gas in the compartment can be determined by integrating the normalized form of Eq. 3 to give

$$\Pi'(t) - \Pi'(0) = \lambda Q \int_0^t (\Pi'_a - \Pi'_v)dt. \tag{6}$$

The integral term in Eq. 6, to be denoted by ϵ, can be evaluated numerically from the arterial and mixed venous gas tension measurements. If the uptake of inert gas proceeds to saturation, then

$$\epsilon = (\lambda Q)^{-1}. \tag{7}$$

The experimental data were normalized to conform to the ideal conditions defined by Eqs. 4 and 5. The values of ϵ, 8.693 min for *He* uptake and 14.368 min for N_2 uptake, were obtained from the difference between the arterial and venous gas tension measurements for the two groups of rabbits. These values of ϵ can be checked for physical correctness through the use of Eq. 7. Since the blood perfusion rate, Q, is independent of the inert gas used, the following expression for the ratio of the compartment solubilities of N_2 to *He* can be obtained:

$$L(N_2)/L(He) = L_b(N_2)\epsilon(N_2)/L_b(He)\epsilon(He) \tag{8}$$

The experimentally-determined value of this ratio is 2.47 (see APPENDIX for gas solubility data). This value lies between that of water, with a ratio of 1.44, and that of olive oil, with a ratio of 4.52, thereby suggesting that the single compartment used to model gas uptake in the rabbit has solubility characteristics similar to a composite of these two fluids.

The uptake of inert gas in the compartment was calculated through Eq. 6 with the values of λQ determined by Eq. 7. Results are given in Fig. 4a for *He* uptake and in Fig. 4b for N_2 uptake. Note that in the case of *He* uptake, the compartment gas tension lags behind the measured mixed venous blood gas tension. This finding indicates that for *He* uptake, the single compartment is not perfusion-limited, otherwise Π' would equal Π'_v at all times. However, in the case of N_2 uptake, closer agreement between the compartmental gas tension and the measured mixed venous blood gas tension is found, indicating that, at least for this inert gas, perfusion-limitation is a good approximation for the single compartment model. Therefore, although this model is satisfactory for describing N_2 uptake, it is too simplistic to accurately predict the rate of *He* uptake in the whole animal.

Two-Compartment Model

In 1945, Behnke (19) examined the exchange of inert gases in relation to the fat and water content of body tissues. The concept of partitioning the body tissues into two compartments is adopted here and is shown schematically in Fig. 3b. The fat component, designated by the subscript f, is conventionally modelled by olive oil because of its high solubility for gas. The non-fat component, designated by the subscript nf, is modelled by water.

The rate of change of the total gas mass for the two components is expressed by the differental equation

$$dM = dM_f + dM_{nf}. \tag{9}$$

If α is defined as the fractional volume of the fat component, then upon dividing by the sum of fat and non-fat volumes, Eq. 9 becomes

$$dM/V = \alpha dM_f/V_f + (1-\alpha)dM_{nf}/V_{nf}. \tag{10}$$

By applying the Ostwald solubility coefficient and equating Eq. 10 to Eq. 2, the following differential equation relating the measured blood gas tensions to the compartmental gas tensions is obtained:

$$L_b Q(\Pi_a - \Pi_v)dt = \alpha L_f \, d\Pi_f + (1-\alpha)L_{nf} \, d\Pi_{nf}. \tag{11}$$

For the case of complete saturation of the compartments, defined in normalized form by Eq. 5, the integration of the normalized form of Eq. 11 gives

$$L_b Q\epsilon = \alpha L_f + (1-\alpha)L_{nf}. \tag{12}$$

Equation 12 can be applied separately to each inert gas and the two resulting equations can then be combined to give the following expression for the fractional volume of fat:

$$\alpha = \frac{L_{nf}(He)L_b\epsilon(N_2) - L_{nf}(N_2)L_b(He)\epsilon(He)}{[L_f(N_2) - L_{nf}(N_2)]L_b(He)\epsilon(He) - [L_f(He) - L_{nf}(He)]L_b(N_2)\epsilon(N_2)}. \quad (13)$$

The value of the overall blood perfusion rate is then evaluated directly from Eq. 12. The values of α and Q can then be compared to measured physiological data.

If the non-fat component of the model volume is considered to be comprised of both the visceral components and the lean tissues, and the fat component of only the fat tissues, then the expected values of α and Q from the physiological data given in the APPENDIX are 0.144 and 0.114 (*ml* blood/ *ml* tissue) min^{-1}, respectively. The experimentally-determined values, 0.232 for α and 0.132 for Q, overpredict the expected physiological values, especially in the case of the fractional volume of fat. Closer agreement may be attained by considering the whole body fat composition, that is, by including the fatty substances of the visceral components and of the lean tissues. Also, the overprediction in the values of α and Q may be due, in part, to the assumption of complete saturation of the compartments and from the estimation of the arterio-venous difference in gas tension obtained from measurements between two different groups of rabbits. In order to avoid these difficulties, it is necessary to examine a higher-order model.

Four-Compartment Model

Palazzi et al. (20) have recently developed a four-compartment model appropriate for this analysis. It is based on an analytical solution of mass conservation for the uptake of inspired inert gases that includes the exchange of gas between the lungs and blood. The four compartments, shown schematically in Fig. 3d, represent the alveolar region, the visceral components, the lean tissues, and the fat tissues. Of the various assumptions used in the four-compartment model, the following are noteworthy:

i) a constant inspired gas pressure,

ii) equilibrium of the inert gas tension between the compartment and the venous blood (perfusion-limitation approximation), and

iii) a blood circulation time of zero.

The mass conservation equation for the exchange of gas between the alveolar region and the blood is given by (20)

$$Q_1(C_* - C_1)dt + Q_*(C_* - C_*)dt = V_1 dC_1, \quad (14)$$

where Q_1 is rate of alveolar ventilation, C_* is the inspired gas concentration, C_1 is the gas concentration in the alveolar region, Q_* is the volumetric blood flow rate to the lungs, and V_1 is the lung volume. For each of the remaining three compartments, the mass conservation equation is given by

$$Q_i(C_* - C_i)dt = V_i\, dC_i. \quad (15)$$

The four-compartment model was applied to predict the arterial and mixed venous blood gas tensions in the rabbit for the experimental conditions outlined earlier. The physiological parameters that have been used to model the various compartments of the rabbit are outlined in the APPENDIX. Gas solubility in the visceral components was assumed to have the value for blood and that for the lean tissues by water. According to the four-compartment model, the arterial gas tension predicted for both *He* and N_2 uptake is essentially the same and is shown in Fig. 5 to reach 99% saturation within two minutes of exposure. This is much faster than the measured times of 17 min for *He* and 55 min for N_2, also shown in Fig. 5.

There is also poor agreement between the measured values with the predicted values for both *He* and N_2 uptake in the mixed venous blood, as shown in Fig.5. Varying certain physiological parameters such as blood perfusion rates and gas solubility does not improve the agreement significantly. It is uncertain where the model fails except to suggest that perhaps the saturation rate at the arterial level and subsequently the rate of inert gas uptake in the venous blood is reduced by shunting of blood at the lung level or by depressing spontaneous ventilation

as the result of not artifically ventilating the anesthetized animals.

An alternative approach to explain the experimental result is to use the conservation of mass method to predict the mixed venous gas tensions directly from the measured arterial values. In this way, the assumptions of constant inspired gas pressure and zero blood circulation time, used in the four-compartment model, are removed.

Three-Compartment Model

Since the alveolar region can be bypassed by using the measured arterial values directly, a three-compartment model, shown schematically in Fig. 3c, might be more applicable than the four-compartment model used previously. Accordingly, this analysis begins with the mass balance equation written for the i^{th} compartment (21)

$$Q_i(C_a - C_i)dt = V_i\,dC_i + V_{bi}\,dC_{bi} \tag{16}$$

where the subscript, bi, refers to a property of the blood of the i^{th} compartment. This equation is essentially the same as Eq. 15 except for the inclusion of blood volumes. In essence, Eq. 16 states that the difference in gas content between the arterial and venous sides is taken up in the compartment volume. After dividing Eq. 16 by the compartment volume, V_i, and applying the Ostwald solubility coefficient, Eq. 16 becomes

$$L_b\,Q_i(\Pi_a - \Pi_{vi})dt = L_i\,d\Pi_i + L_b(V_{bi}/V_i)d\Pi_{bi}, \tag{17}$$

where the subscript, vi, refers to a property of the venous blood of the i^{th} compartment. This mass balance equation can be further simplified by defining the fraction of blood volume by $\beta_i = V_{bi}/V_b$ and by applying the perfusion-limitation approximation, i.e. $\Pi_i = \Pi_{vi}$; then after some rearrangement, Eq. 17 becomes

$$d\Pi_{vi} = \lambda_i\,Q_i(\Pi_a - \Pi_{vi})dt - \lambda_i\,\beta_i(V_b/V_i)d\Pi_{bi}. \tag{18}$$

The inert gas tension in the venous blood of each compartment, Π_{vi}, can be evaluated numerically through Eq. 18. The inert gas tension in the blood of the i^{th} compartment, Π_{bi}, is approximated by the mean of the measured arterial values and the predicted venous values for that compartment. Finally, the mixed venous gas tension is determined from the identity

$$\Pi_v = \sum_{i=1}^{3} \beta_i \Pi_i. \tag{19}$$

Equation 19 can be used to predict the mixed venous gas tension for the group of rabbits for which the arterial gas tension was measured. This prediction can then be compared with the mixed venous gas tension measured for the second group of rabbits. The predicted and averaged measured values of the mixed venous blood gas tension are shown in normalized form in Fig. 6a for *He* uptake and in Fig. 6b for N_2 uptake. These figures also show the predicted uptake of inert gas tension in the three compartments.

Good agreement between the predicted and the measured values of the mixed venous gas tension for *He* uptake suggests that the model used here is a reasonable one. The uptake of *He*, shown in Fig. 6a, is highest for the visceral component and is lowest for the fat tissue. This is expected in a perfusion-limited system where the fat tissue is less perfused by blood than are the visceral components.

There is, however, poor agreement between the predicted and the measured values of the mixed venous gas tension for N_2 uptake as shown in Fig. 6b. While it appears that the perfusion-limited approximation is valid for *He* uptake, the validity of this approximation for N_2 uptake is in doubt.

The diffusivity of N_2 is slower than *He* in aqueous solution (22), therefore, the exchange of N_2 between blood and tissue may be diffusion-limited. This would lead to a slower tissue saturation rate and therefore the retention of N_2 in the arterial blood should result in mixed venous blood gas tension values larger than that predicted by the perfusion-limitation approximation.

Since the mixed venous blood N_2 tension predicted by the perfusion-limitation approximation already exceeds the measured values, the possibility of diffusion-limitation is remote. This leaves the physiological data in question.

Of the various parameters used, the gas solubility coefficient is subject to the greatest variability. For lack of better data, the conventional assumption of modelling the gas solubility coefficient for lean tissue by water and that for fat tissue by olive oil was applied (see APPENDIX). Varying these two coefficients does not alter the result substantially. In the case of the visceral component, a gas solubility coefficient is chosen whose value is the same as in blood (no measured data are available in this case). Increasing the N_2 solubility coefficient in the compartment that models the visceral component will reduce the predicted mixed venous blood gas tension as indicated by the dashed line in Fig. 6b., but not sufficiently for agreement with the measured values. Until better gas solubility data become available, it is difficult to judge the validity of the three-compartment perfusion-limitation model for N_2 uptake between tissue and blood.

DISCUSSION

The long saturation period measured for both *He* and N_2 in the arterial blood (see Fig. 2) is contrary to the usual assumption of instantaneous equilibriation of inert gases in the pulmonary capillary blood (23). This result cannot be explained by the short time delay in the response to the presence of either *He* or N_2, of the catheter of the mass spectrometer probe. This is because the short time delays in the response to these gases (see METHOD) do not contribute significantly to the measured saturation rates, as determined by methods described elsewhere (24). The slow saturation rates of these inert gases in the arterial blood may be due to shunting of blood, as discussed in greater detail elsewhere (25) or to depressing spontaneous ventilation as a consequence of anesthesia. In these experiments, artificial ventilation was not applied.

The cross-over of uptake rates in the mixed venous blood between *He* and N_2 (see Fig. 2) was unexpected since the solubility of *He* in biological fluids and tissue is lower than for N_2 (18) and, therefore, less *He* should be required to saturate the body. The rate of gas uptake with *He* should therefore be faster than with N_2. The reason for this anomaly is not clear but may be due, in part, to inert gas diffusion through the animal's skin; i.e., while the animal is inspiring the breathing mixture containing *He* , a gradient is established for the elimination of *He* through the skin into the chamber atmosphere which contains no *He* . Therefore, a longer saturation period for *He* may be required as shown in Fig. 2.

Also, during inspiration of the chamber gas mixture, the presence of N_2 in the chamber atmosphere may enhance the N_2 saturation rate in the animal's body through the same process of gas diffusion through the skin, but in the reverse direction. The diffusion of N_2 through the skin has been previously observed (26). The magnitude of this effect in the experiments described here is difficult to ascertain since the amount of N_2 diffusing through the skin cannot be separated from the contribution of N_2 washin during the phase of N_2 uptake or of N_2 washout from slow tissues during the phase of *He* uptake.

Another possible explanation of the cross-over effect may be due to a removal of *He* from the dissolved state to a gaseous state through bubble formation. It has been reported (17,27,28) that the isobaric switching of inhaled gases from N_2 to *He* creates a condition of gas supersaturation. Therefore, when switching the breathing mixture for the rabbits from 90% N_2 and 10% O_2 to 90% *He* and 10% O_2, there is the possibility of a total gas supersaturation leading to bubble formation in the mixed venous blood. The removal of dissolved *He* through this phase change could account for a lowering of the rate of *He* saturation in the mixed venous blood.

SUMMARY

Several rabbits were exposed to hyperbaric breathing mixtures containing either *He* or N_2 in an attempt to measure the rates of uptake of these gases in the animal's blood and tissues. The use of mass spectrometry provided a direct and continuous means of measuring the inert gases dissolved in the blood. However, blood sampling could only be taken from either the arterial or venous side. Thus, the arterio-venous difference in inert gas tension could not be measured directly and therefore this difference could only be approximated by taking the mean values between the two groups of rabbits.

To analyze the rate of inert gas exchange, various compartmental models were applied. The one-compartment model appeared to be suitable for N_2 uptake between blood and tissue, and demonstrated that the uptake may be perfusion-limited. However, this model was not suitable for *He* uptake. The two-compartment model is physically more realistic than the one-compartment model; however, it was found to be unsuitable since the experimentally-determined fractional volume of fat was unrealistically high. The four-compartment model of Palazzi et al. (20) was also not suitable since it did not predict the relatively slow rate of inert gas uptake in the arterial blood, nor the correct rates of inert gas uptake in the mixed venous blood. Alternatively, the three-compartment model, which bypasses the alveolar region, was found to be appropriate for predicting the whole body uptake of *He* in the anesthetized rabbit.

RECOMMENDATIONS

To measure the arterio-venous difference in inert gas tension directly, the implantation of two mass spectrometer probes, one in the arterial blood and one in the venous blood, should be considered for future studies. In this way, each animal could be examined separately and the physiological variations between the animals would be eliminated for a more exact analysis of inert gas exchange.

The models of inert gas uptake used in this study did not include features as blood shunting, possible bubble formation, counter-current gas exchange between the arterial and venous blood, and gas diffusion through the skin since the physical and physiological data to support the implementation of these features are not available. As the data for these features become available, they should be implemented into the models of inert gas uptake.

ACKNOWLEDGMENTS

The authors gratefully acknowledge the constructive comments kindly given by Dr. Richard D. Vann of Duke University Medical Center in the preparation of this paper. The study was done under the Franco-Canadian Accord with the experimental work being done at the Centre d'Etude et de Recherches Biophysiologique Appliquée à la Marine, Toulon, France and the analytical work being done at DCIEM.

REFERENCES

1. Boycott AE, Damant GCC, Haldane JS. The prevention of compressed air illness. J Hygiene 8:342-443, 1908.
2. Jones HB. Gas exchange and blood-tissue perfusion factors in various body tissues. In: Fulton JF, ed. Decompression sickness. Philadelphia: Saunders, 278-321, 1951.
3. Kety SS. The theory and application of the exchange of inert gas at the lungs and tissues. Pharmacol Rev 3:1-41, 1951.
4. Roughton FJW. Diffusion and chemical reaction velocity in cylindrical and spherical systems of physiological interest. Proc R Soc B140:203-221, 1952.
5. Harvey CA, Lambersten CJ. Deep-tissue isobaric inert gas exchange: Predictions during normoxic helium, neon, and nitrogen breathing at 1200 fsw. In: Shilling CW, Beckett MW, eds. Underwater physiology VI. Bethesda: Federation of American Societies for Experimental Biology, 343-357, 1978.
6. Hills BA. Decompression sickness: The biophysical basis of the prevention and treatment. New York: John Wiley and Sons, 167-181, 1977.
7. Morales MF, Smith RE. On the theory of blood-tissue exchange of inert gases: VI Validity of approximate uptake expressions. Bull Math Biophysics 10:191-200, 1948.
8. Weathersby PK, Homer LD. Current concepts of inert gas exchange and decompression. In: Bachrach AJ, Matzen MM, eds. Underwater physiology VII. Bethesda: Undersea Medical Society Inc, 687-698, 1981.
9. Hills BA. Vital issues in computing decompression schedules from fundamentals: II. Diffusion versus perfusion in controlling blood:tissue exchange. Int J Biometeor 14:323-342, 1970.
10. Hennessy TR. The interaction of diffusion and perfusion in homogeneous tissue. Bull Math Biol 36:505-526, 1974.
11. Popel AS. Analysis of capillary-tissue diffusion in multicapillary systems. Math Biosciences 39:187-211, 1978.
12. Wald A, Hass WK, Siew FP, Wood DH. Continuous measurement of blood gases in vivo by mass spectrometry. Med Biol Eng 8:111-128, 1970.
13. Weathersby PK, Mendendall KG, Barnard EEP, Homer LD, Survanshi S, Vieras F. Distribution of xenon gas exchange rates in dogs. J Appl Physiol 50:1325-1336, 1981.
14. Albers C, Farhi LE. Analysis of blood gases by gas chromatograhy. In: Mattick LR, Szymanski HA, eds. Lectures on Gas Chromatography. New York: Plenum Press, 163-187, 1965.
15. Giry P, Battesti A, Vernotte M. Mesure des pressions partielles des gaz dissous par spectrométrie de masse - mise au point de sondes à réponse rapide destinées à un usage hyperbare. Centre D'Etudes et de Recherches Bio-Physiologiques Appliquées a la Marine, Toulon, France, Report No.78-07, 1978.
16. Giry P, Servantie B, Meliet JL, Broussolle B. Mesure par specrometrie de masse des pressions partielles de gaz inertes dans le sang artériel au cours de changement de composition des gaz inhalés. Analyze critique de la dyssaturation isobare. Centre D'Etudes et de Recherches Bio-Physiologiques Appliquées a la Marine, Toulon, France, Report No.80-07, 1980.
17. Giry P, Broussolle B. Mesure par spectrométrie de masse pressions partielles de gaz inertes dans le sang vieneux au cours de changement de composition de gaz inhales a 5 ATA. Centre D'Etudes et de Recherches Bio-Physiologiques Appliquées a la Marine, Toulon, France, Report No.80-12, 1980.
18. Weathersby PK, Homer LD. Solubility of inert gases in biological fluids and tissues: a review. Undersea Biomed Res 7:277-296, 1980.

19. Behnke AR. The absorption and elimination of gases of the body in relation to its fat and water content. Medicine 24:359-379, 1945.

20. Palazzi E, Rovatti M, Del Borghi M, Peloso A. n-compartment mathematical model for the uptake and distribution of inhaled inert gases in the human body: an analytical solution. Med Biol Eng Comp 21:128-133, 1983.

21. Cooney DO. Biomedical engineering principles. New York: Marcel Dekker Inc, 203-206, 1966.

22. Wise DL, Houghton G. The diffusion coefficients of ten slightly soluble gases in water at 10-60 ° C. Chem Eng Sci 21:999-1010, 1966.

23. Forester RE. Diffusion of gases. In: Fenn WO, Rahn H, eds. Handbook of physiology respiration. Washington: American Physiological Society, 844-845, 1964.

24. Nishi RY, Holness DE, Sweeney DM. Mathematical correction of data for the lag-response of teflon catheters used in mass spectrometry. In: Holness DE, Ackles KN, eds. Problems and Solutions in the use of Mass Spectrometry in Hyperbaric Environments. Defence and Civil Institute of Environmental Medicine, Downsview, Ontario, Canada, Report No. 76-X-28, 1976.

25. Giry P, Broussolle B, Meliet J-L, Monti M. Variations de la somme des pressions partielles arterielles des gaz inertes au cours de changements de composition des gaz inhales sans variation de pression ambiante en atmosphere hyperbare. C R Acad Sc Paris 292:335-338, 1981.

26. Ackles KN, Holness DE, Brock AJ. Tissue, blood and respiratory nitrogen responses during compression on Heliox. In: Holness DE, Ackles KN, eds. Problems and Solutions in the use of Mass Spectrometry in Hyperbaric Environments. Defence and Civil Institute of Environmental Medicine, Downsview, Ontario, Canada, Report No. 76-X-28, 1976.

27. Lambersten CJ, Idicula J. A new gas lesion syndrome in man, induced by "isobaric gas counterdiffusion". J Appl Physiol 39:434-443, 1975.

28. D'Aoust BG, Lambertsen CJ. Isobaric gas exchange and supersaturation by counterdiffusion. In: Bennett PB, Elliott DH, eds. The Physiology and Medicine of Diving. San Pedro, California: Best Publishing Co., 383-403, 1982.

29. Kelman GR. Applied cardiovascular physiology. 2nd ed. London: Butterworths, 134, 1977.

30. Kozma C, Macklin W, Cummins LM, Mauer R. Anatomy, physiology, and biochemistry of the rabbit. In: Weisbroth SH, Flatt RE, Kraus AL, eds. The biology of the laboratory rabbit. New York: Academic Press, 56-57, 1974.

31. Altman PL, Dittmer DS. eds. Respiration and circulation. Bethesda: Federation of American Societies of Experimental Biology, 110, 1971.

32. Davidson JT, Wasserman K, Lillington GA, Schmidt RW. Pulmonary function testing in the rabbit. J Appl Physiol 21:1094-1098, 1966.

33. Stahl WR. Scaling of respiratory variables in mammals. J Appl Physiol 22:453-460, 1967.

34. Christoforides C, Hedley-Whyte J. Solubility of N_2O, N_2, and He in human whole blood and water: constant relative solubility of N_2 (abstr). Fed Proc 29:A330, 1970.

35. Behnke AR, Yarbrough OD. Respiratory resistance, oil-water solubility, and mental effects of argon compared with helium and nitrogen. Am J Physiol 126:409-415, 1939.

LIST OF FIGURES

Fig. 1 Schematic of the experimental arrangement showing the rabbit within the hyperbaric chamber.

Fig. 2 Experimentally-observed values of the inert gas tensions in blood, in normalized form, following an isobaric step increase in inspired gas composition. Arterial gas tensions, Π'_a *He* and Π'_a N_2, were averaged from continuous measured values of the gas tension in the aortas of the first group of five anesthetized rabbits. Mixed venous gas tensions, Π'_v *He* and Π'_v N_2, were averaged from continuous measured values of the gas tension in the right atriums of a second group of six anesthetized rabbits. Standard errors of the mean (vertical bars) are only shown for selected mixed venous gas tensions.

Fig. 3 Schematic of the gas exchange models. The external boundaries of the compartments are closed to gas exchange. Gas enters the compartments through the arterial blood and emerges through the venous blood.

Fig. 4 Predicted gas uptake, in normalized form, based on a one-compartment model for the second group of rabbits following a step change in inspired gas composition (He in (a); N_2 in (b)). Selected averaged measured values in the mixed venous blood (•) and their standard error (vertical bars) are shown for comparison.

Fig. 5 Predicted gas uptake, in normalized form, based on a four-compartment model for the arterial blood (ar) and the mixed venous blood (v) of the second group of rabbits following a step change in inspired gas composition (*He* in (a); N_2 in (b)). Selected averaged measured values (•) in the mixed venous blood and their standard error (vertical bars) are shown for comparison.

Fig. 6 Predicted gas uptake, in normalized form, based on a three-compartment model using the measured arterial gas tensions of the first group of rabbits. Predicted values are shown for the mixed venous blood (v), the visceral components, and the lean and fat tissues (*He* in (a); N_2 in (b)). Selected averaged measured values (•) in the mixed venous blood and their standard error (vertical bars) for the second group of rabbits are shown for comparison. The dotted line in (b) is the predicted uptake of N_2 in the mixed venous blood if the gas solubility in the visceral compartment is increased to the value assumed for the fat tissue.

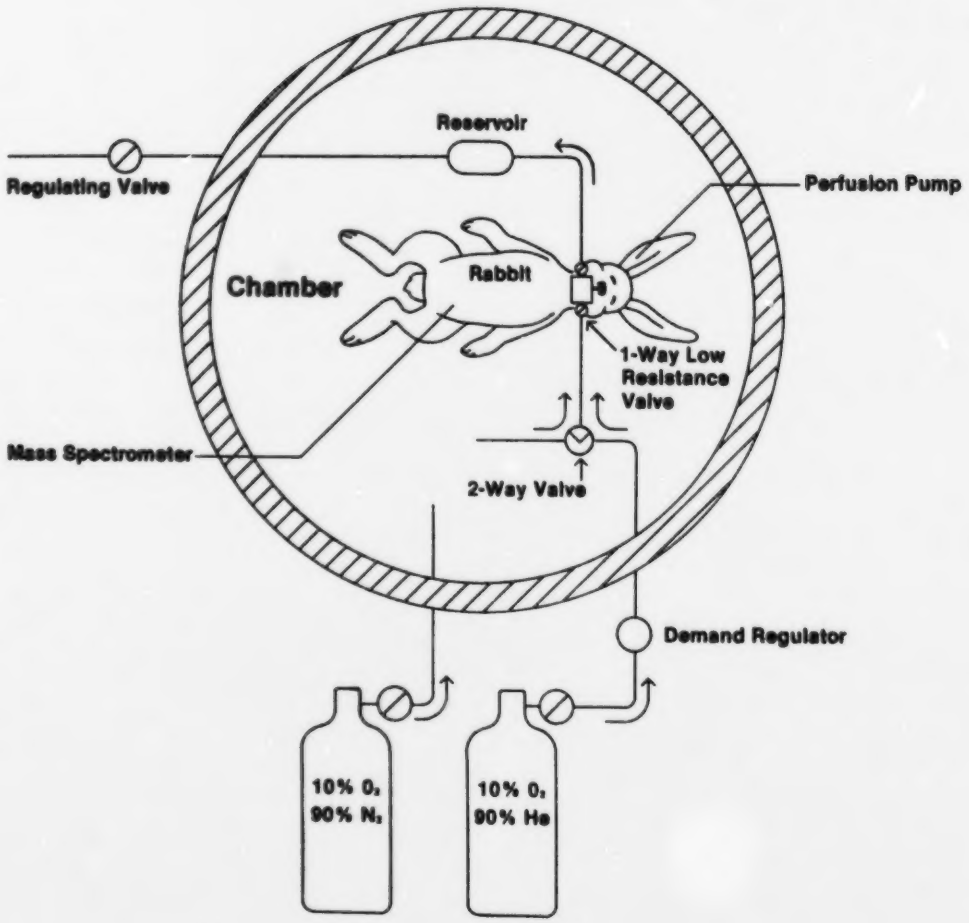

Fig. 1 Schematic of the experimental arrangement showing the rabbit within the hyperbaric chamber.

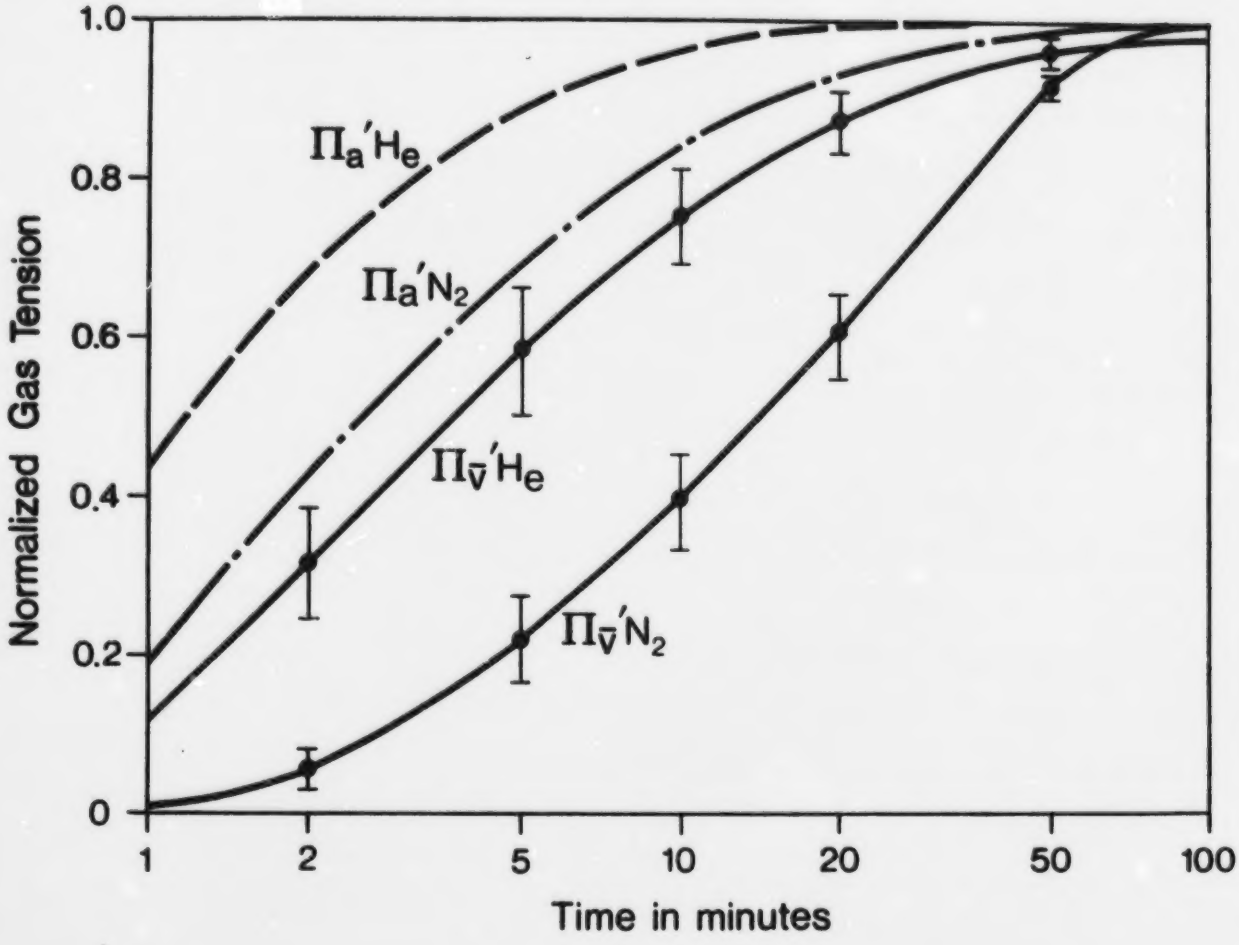

Fig. 2 Experimentally-observed values of the inert gas tensions in blood, in normalized form, following an isobaric step increase in inspired gas composition. Arterial gas tensions, Π'_a *He* and Π'_a N_2, were averaged from continuous measured values of the gas tension in the aortas of the first group of five anesthetized rabbits. Mixed venous gas tensions, $\Pi'_{\bar{v}}$ *He* and $\Pi'_{\bar{v}}$ N_2, were averaged from continuous measured values of the gas tension in the right atriums of a second group of six anesthetized rabbits. Standard errors of the mean (vertical bars) are only shown for selected mixed venous gas tensions.

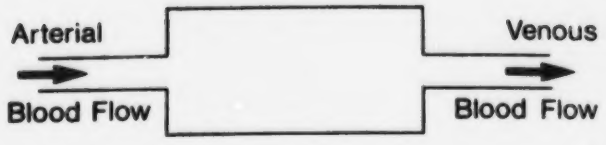

a One - Compartment Model

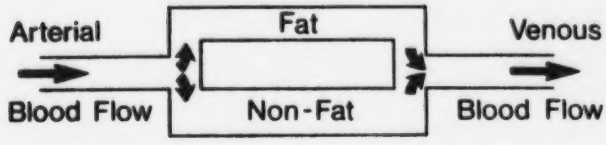

b Two - Compartment Model

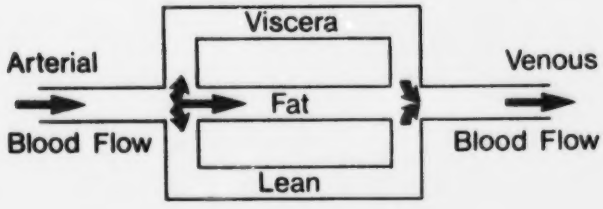

c Three - Compartment Model

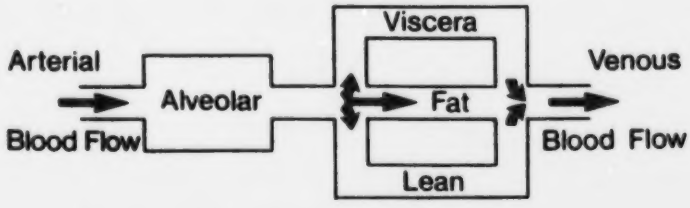

d Four - Compartment Model

Fig. 3 Schematic of the gas exchange models. The external boundaries of the compartments are closed to gas exchange. Gas enters the compartments through the arterial blood and emerges through the venous blood.

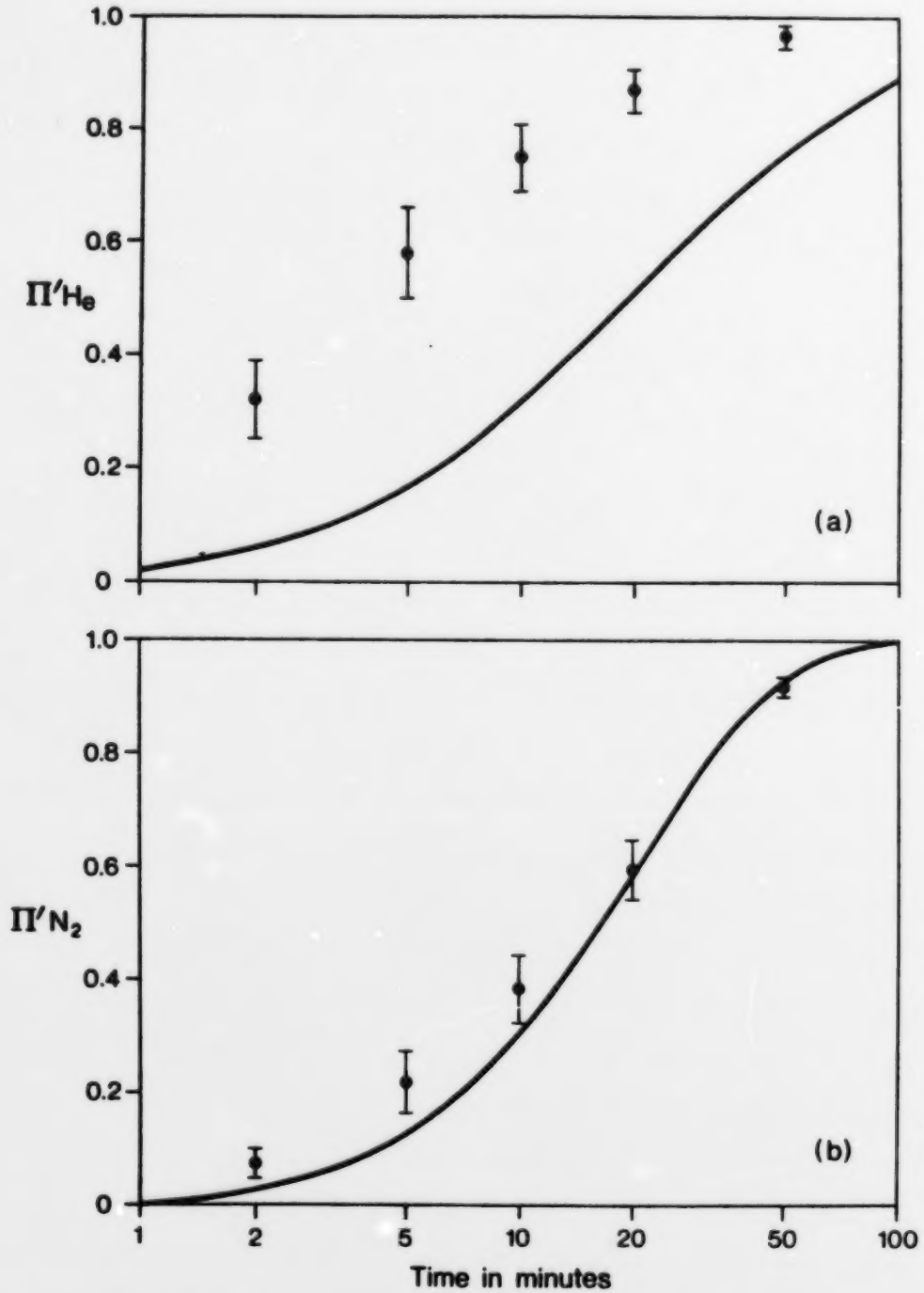

Fig. 4 **Predicted gas uptake, in normalized form, based on a one-compartment model for the second group of rabbits following a step change in inspired gas composition (He in (a); N_2 in (b)). Selected averaged measured values in the mixed venous blood (•) and their standard error (vertical bars) are shown for comparison.**

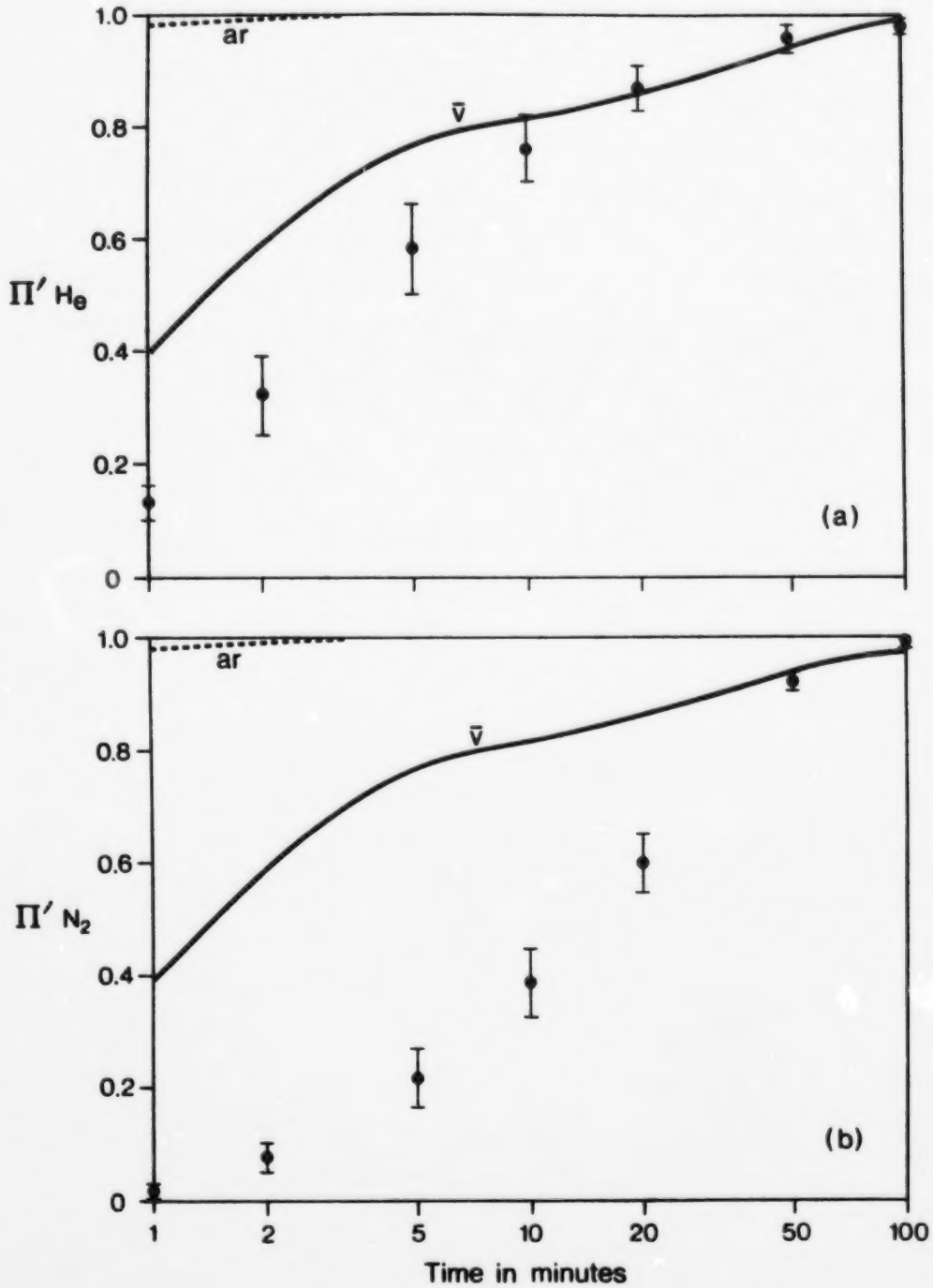

Fig. 5 Predicted gas uptake, in normalized form, based on a four-compartment model for the arterial blood (ar) and the mixed venous blood (v) of the second group of rabbits following a step change in inspired gas composition (*He* in (a); N_2 in (b)). Selected averaged measured values (•) in the mixed venous blood and their standard error (vertical bars) are shown for comparison.

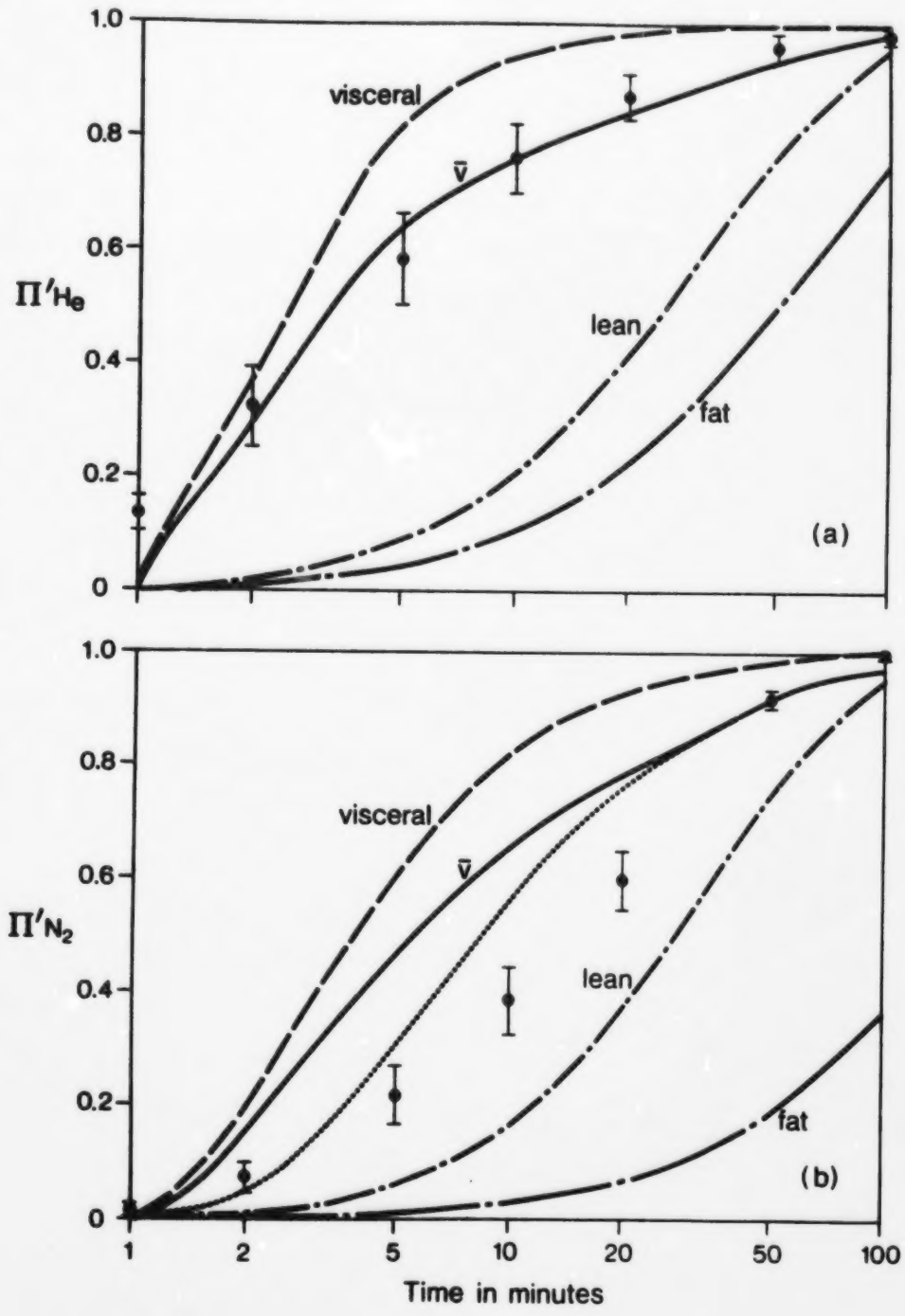

Fig. 6 **Predicted gas uptake, in normalized form, based on a three-compartment model using the measured arterial gas tensions of the first group of rabbits. Predicted values are shown for the mixed venous blood (v), the visceral components, and the lean and fat tissues (*He* in (a); N_2 in (b)). Selected averaged measured values (•) in the mixed venous blood and their standard error (vertical bars) for the second group of rabbits are shown for comparison. The dotted line in (b) is the predicted uptake of N_2 in the mixed venous blood if the gas solubility in the visceral compartment is increased to the value assumed for the fat tissue.**

APPENDIX

Physiological parameters used for the analysis of inert gas uptake in the rabbit

1) Volumes for a 3 kg rabbit

whole body volume	2796 *ml*	assuming specific gravity of 1.073 for man	(29)*
visceral volume	143.5 *ml*	based on mass of 0.0526 kg/kg body mass and specific gravity of 1.099 as based on the lean mass of man	(30) (19)
fat tissue volume	377.5 *ml*	assuming 13.5% fat as based on man	(19)
blood volume	169.4 *ml*		(30)
lean tissue volume	2105.6 *ml*	difference between the whole body volume and the sum of the visceral, fat tissue, and blood volumes	
alveolar volume	57.5 *ml*		(31)

2) Ventilation for a 3 kg rabbit

alveolar ventilation	278.4 *ml* min^{-1}	based on a minute volume of 570 *ml*,	(32)
		a respiration rate of 36.8 min^{-1},	(32)
		and a dead space of 7.92 *ml*	(33)

3) Volumetric blood flow rates for a 3 kg rabbit

for lean tissue	63.6 *ml* min^{-1}	assuming a lean tissue blood perfusion rate of 0.0302 (*ml* blood/ *ml* tissue) min^{-1} as based on man	(29)
for fat tissue	8.87 *ml* min^{-1}	assuming a fat tissue blood perfusion rate of 0.0235 (*ml* blood/ *ml* tissue) min^{-1} as based on man	(29)
for visceral components	227.5 *ml* min^{-1}	difference between overall blood flow rate and the sum of blood flow rates of the lean and fat tissues, assuming an overall blood flow rate of 300 *ml* min^{-1}	

4) Ostwald gas solubility coefficients at 37 ° C

	for *He*	for N_2	
in blood	0.0104	0.0158	(34)
in water	0.0101	0.0145	(34)
in olive oil	0.0168	0.0760	(35)

* Numbers in parenthesis are reference numbers